applied sciences

MDPI

Article

# Chitosan Microbeads as Supporter for *Pseudomonas putida* with Surface Displayed Laccases for Decolorization of Synthetic Dyes

**Zhiqiang Bai [1,2], Xiaowen Sun [1], Xun Yu [1] and Lin Li [1,*]**

[1] State Key Laboratory of Agricultural Microbiology, College of Life Science and Technology, Huazhong Agriculture University, Wuhan 430070, China; baizq1987@126.com (Z.B.); sunxiaowen525@webmail.hzau.edu.cn (X.S.); yuxun@webmail.hzau.edu.cn (X.Y.)

[2] School of Life Sciences, Shanxi Datong University, Datong 037009, China

* Correspondence: lilin@mail.hzau.edu.cn; Tel.: +86-27-8728-6952

Received: 3 December 2018; Accepted: 24 December 2018; Published: 3 January 2019


**Abstract:** Various untreated wastewaters contaminated with industrial dyes pose significant pollution hazards to the natural environment as well as serious risks to public health. The current study reports a new material with a configurative chitosan matrix and engineered *Pseudomonas putida* cells with surface-displayed laccases that can decolorize five industrial dyes. Through a self-configuring device, five chitosan microbeads (CTS-MBs) with different particle sizes were prepared. *P. putida* cells were then immobilized onto the CTS-MBs under optimized immobilization conditions, forming a degrading-biosorbent dual-function decolorization complex. Scanning electron microscope and infrared analysis confirmed the successful immobilization of the cells onto the CTS-MB matrix. The optimized CTS-MB1 with surface-grafted aldehyde groups (aCTS-MB1) complex was capable of decolorizing Acid Green 25 and Acid Red 18 over a pH range of 2.5–8.5 and a relatively broad temperature range of 15–85 °C, with a maximum relative decolorization value of over 94%; the complex was also able to efficiently decolorize Direct Red 243, Reactive Blue 220 and Reactive Blue 198. Moreover, the aCTS-MB1 composite showed favorable activity in continuous and regenerative decolorization reactions. Therefore, the chitosan-immobilized decolorizing material, with both improved mechanical strength and performance, shows potential for further large-scale or continuous processes.

**Keywords:** chitosan; *Pseudomonas putida*; immobilization; dye decolorization; degradation; biosorption

## 1. Introduction

Textile dyes comprise a large class of chemicals with highly comprehensive components, diverse origins and extensive applications and they constitute the main source of pollution in sewage discharge from the textile and printing industry. In China and Southeast Asia, contamination caused by various textile dyes from untreated industrial effluents is a serious environmental threat, as a variety of textile dyes are toxic or cross-coupled to toxic components that are relatively recalcitrant to degradation due to their complicated molecular structure [1,2]. Even a small amount of trace dye in water can seriously affect the transparency and gas solubility of the water [3]. Remediation of dye contamination often involves chemical, physical and various biological processes [4,5]. Over the past decade, intensive efforts have been made to develop effective bioprocesses for the treatment of dyes in wastewater effluents or other environments [2,6]. Of the various available biological decolorizers, the macromolecular polymer chitosan (CTS) has particular appeal due to its relatively high natural dye biosorption efficiency and its ease of transformation into biocomposites through physicochemical modification, which leads to efficient decolorization of various dyes [7–9].

CTS is a natural poly-amino glucosamine polymer that is widely distributed in the exoskeleton of various crustaceans, in the exo- and endocuticle of insects and in the cell wall of fungi, where it functions as an integral component as well as a mechanically strong supporting scaffold material for these organisms; moreover, CTS has been recognized as one of the most plentiful renewable organic resources worldwide [10,11]. The distinctive biological properties of CTS, particularly its biocompatibility, biodegradability, environmental friendliness and regenerability, as well as its relative permeability and cost-effectiveness, indicate its potential for applications in a variety of industrial fields, such as biochemical engineering, wastewater remediation, food processing [12,13], bone tissue engineering and other therapeutic applications [14,15].

In addition to biosorption, enzymatic biodegradation provides another promising approach to the decolorization of wastewater dyes [16]. Among various degrading enzymes such as phenoloxidases, laccases and tyrosinases, microbial laccases are being increasingly investigated as an effective and environmentally friendly means of treating industrial phenolic substrates [17]. Laccases (benzenediol:dioxygen oxidoreductases, EC1.10S.3.2) are a large group of multi-copper enzymes that are involved in different biological processes of organisms, such as lignifications in plants; morphogenesis, pathogenesis and detoxification in fungi; cuticle osteosis; and resistance to heave metals, chlorides, ultraviolet (UV) radiation and $H_2O_2$ in bacteria, among others [16,18,19]. Many previous investigations have demonstrated the ability of microbial laccases to oxidatively degrade a broad range of organic compounds, particularly aromatic substrates [20–22], including industrial or wastewater dyes [17,23,24]. In a similar approach, we developed a *Pseudomonas* cell surface display system to efficiently decolorize the anthraquinone dye Acid Green 25 and diazo dye Acid Red 18 [25] in which a mutated bacterial laccase (WlacD) [26] was projected onto the surface of target cells, enabling fast and goal-oriented decolorization on the cell surface. This system has proven advantages over freely suspended laccase and bacterial cells alone, including the elimination of mass transfer limitation, minimization of dye toxicity to living cells and particularly, promotion of the reaction rate. However, one technical drawback remained in this system: its inability to be applied in large-scale or continuous processes, as high loading of this type of biomass, which is composed of cells, will become clogged under continuous-flow conditions in a reactor. In addition, as a recombinant bacterial strain, carrying an antibiotic marker is also an important concern for environmental release. Therefore, further studies to improve the performance of this system for large-scale or continuous operations are required.

*Pseudomonas putida* is a well-known non-pathogenic and robust bacterium, with a wealth of oxidoreductases and a versatile metabolism capable of utilizing a wide range of inorganic and organic compounds [27,28]. Moreover, this bacterium exhibits a high tolerance towards harsh environmental conditions and can live in various environmental niches [28], rendering it a valuable host for treating wastewater pollutants. On the other hand, the ease of preparing various CTS matrices by cross-linking modifications has been established due to its good hydrophilicity, mechanical stability and degree of rigidity [29,30]. The immobilization or embedding of various dye-degrading enzymes or cells with dye-degrading or dye-adsorptive capability on CTS leads to increased decolorization efficiency through the increased pores on the surface of CTS beads [31] or immobilized enzymes/cells [30]. To further improve the performance of our laccase-based cell surface display system in terms of decolorization efficiency, stability and applicability for large-scale or continuous processes, in the present study, using a self-configuring device, a facile and applicable CTS-microsome preparation system was self-assembled and used to prepare five CTS microbead (CTS-MB) materials with different microsome sizes from a pulverous CTS substrate. The CTS-MBs were then used to immobilize engineered *P. putida* MB285 cells with surface-displayed laccase to construct a "CTS-MB/*P. putida* MB285 cell" biosorbent/biodegrading dual-function system. The effects of temperature, pH and storage time on the laccase activity of the optimal complex were investigated. The interactions between the CTS-MBs and *P. putida* cells were examined using scanning electron microscopy (SEM) and Fourier transform infrared (FT-IR) spectroscopy. The material was then used to decolorize five synthetic

dyes and its decolorization efficiency together with its capability during 10 rounds of continuous decolorization and 6 cycles of re-culturing were investigated.

## 2. Materials and Methods

### *2.1. Chemicals, Bacterial Strains and Culture Conditions*

Analytical-grade CTS was purchased from Sinopharm Chemical Reagent Co., Ltd. (Wuhan branch, China). According to the manufacturer's product manual, this off-white translucent powder product is a water-insoluble but dilute acid-soluble polymer with a chemical formula of $(C_6H_{11}NO_4)_n$, an average molecular weight of $6.2 \times 10^5$ Da and a degree of deacetylation of $\geq$90.0%. Five industrial-grade dyes (Table S1) that belonging to four structural categories were used for the decolorization experiments: azo dyes Acid Red 18 (AR18) and Direct Red 243 (DB243), anthraquinone dye Acid Green 25 (AG25), phthalocyanine dye Reactive Blue 220 (RB220) and tribenyldioxazine dye Reactive Blue 198 (RB198). Among these dyes, AG25 and AR18 were purchased from Thailand Modern Destuffs & Pigments Company (Lardpraw 94, Bangkok, Thailand) and RB198, RB220 and DR243 were purchased from Jinsheng Dyestuff Chemical Co., Ltd. (Jinan, China). Other chemical reagents were purchased from Sinopharm Chemical Reagent Co., Ltd. and were of analytical grade. The recombinant *P. putida* MB285 strain [21] was routinely grown at 28 °C in lysogeny broth (LB) medium [32] containing 500 μg $mL^{-1}$ (final concentration) of carbenicillin.

### *2.2. Preparation of CTS-MBs*

The technical process for preparing the CTS-MBs with surface-grafted aldehyde groups (i.e., the activated CTS-MBs, aCTS-MBs in brief) and the complex with immobilized *P. putida* cells (i.e., the aCTS-MBs complexed with *P. putida* cells, bacCTS-MBs in brief) is illustrated in Figure 1. First, 2 g of CTS powder was dissolved in 100 mL of a 1% (*v*/*v*) acetic acid solution, followed by vigorous stirring with a magnetic stirrer for at least 12 h. To prepare CTS-MB with different particle sizes, we designed and self-assembled a set of facile preparation devices consisting of a constant flow pump, a DC high-voltage power supply (HV-PS), a magnetic stirrer and a medical needle (30 G) that was placed at a height of 3.5 cm over a NaOH-ethanol solution (Figure S1). The negative electrode of the HV-PS was connected to a copper ring that was immersed in a NaOH-ethanol solution and the positive electrode of the HV-PS was connected to a needle. CTS-MBs formed in the NaOH-ethanol solution when the CTS solution was titrated from the needle at a flow rate of 0.05 mL $min^{-1}$ and was stirred at 200 rpm. By adjusting the voltage of the HV-PS from 5.3 kV to 0 kV, five CTS-MB preparations with particle diameters ranging from 450 μm to 2100 μm were made. For each, the collected CTS-MBs were washed with double distilled water ($ddH_2O$) to remove NaOH.

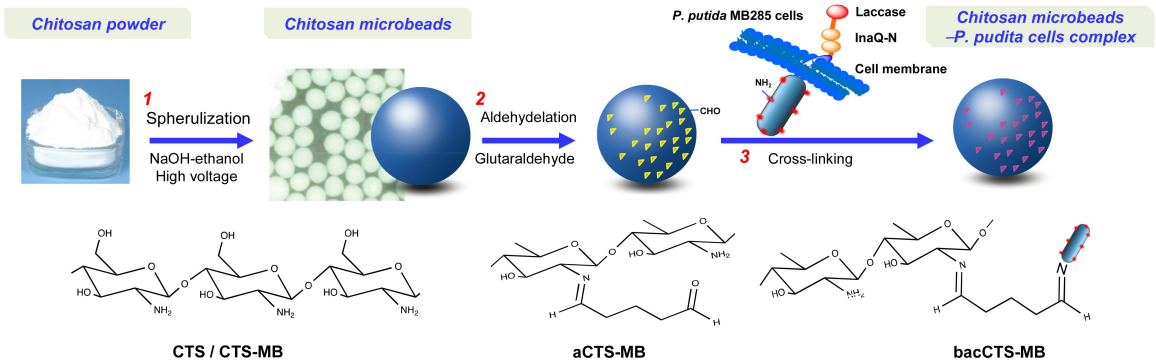


**Figure 1.** Schematic illustration showing the preparation of the bacCTS-MB complex. 1, Preparation of the CTS-MBs; 2, Surface grafting of aldehyde groups on the CTS-MBs (aCTS-MBs); 3, Immobilization of *P. putida* MB285 cells onto the aCTS-MBs via covalent cross-linkages to prepare the bacCTS-MB materials.

### 2.3. Surface Aldehyde Modification of the CTS-MBs and Immobilization of P. putida MB285 Cells

To prepare the aCTS-MBs, 2 g of each of the above CTS-MB preparations were dispersed and suspended in 10 mL of 8% glutaraldehyde. Each suspension was shaken for several minutes and modified CTS beads with surface-grafted aldehydic groups were then obtained by centrifugation and washing with $ddH_2O$.

To immobilize *P. putida* cells onto the aCTS-MB materials, an overnight culture of *P. putida* MB285 cells (approximately $1 \times 10^{10}$ cells $mL^{-1}$) was harvested, washed three times with sterile phosphate-buffered saline (PBS) (pH 7.4) and diluted to a unit cell density ($OD_{600}$ of 5.0) using PBS buffer (pH 7.4) to make a stock cell suspension. Subsequently, 100 mL of the MB285 cell suspension and an appropriate amount of each aCTS-MB material were added to a 250-mL Erlenmeyer flask (enough to fully immerse the material in the cell suspension). Each mixed suspension was then incubated with agitation at 60 rpm to prepare a complex with CTS-MBs crosslinked by *P. putida* MB285 cells. The crosslinking reaction temperature ranged from 4 °C to 36 °C, the reaction time from 2 h to 12 h and the glutaraldehyde concentrations from 0.5% to 8%. The five prepared CTS-MB materials were subjected to an orthogonal trial ($L_{25}$, $4^5$) to optimize the reaction conditions for the immobilization of *P. putida* cells on the CTS-MB materials. The prepared bacCTS-MB materials were washed with sterile PBS buffer (pH 7.4) to remove non-crosslinked cells and residual glutaraldehyde and were then stored at 4 °C until use.

### 2.4. Assay of IBCC-B Enzymatic Activity

The laccase enzymatic activity of the complexes was measured using 2,2′-azino-bis(3-ethyl-benzthiazoline-6-sulfonic acid) (ABTS) (Amresco) as the substrate at 25 °C, according to a previously described method [22] with minor modifications. Basically, 2 g of each bacCTS-MB complex was added to the reaction system (10-mL total volume), which contained 0.1 mol $L^{-1}$ sodium acetate buffer (pH 2.5), 0.5 mmol $L^{-1}$ ABTS and 2 mmol $L^{-1}$ $CuCl_2$. The ABTS oxidation rate was calculated based on the net increase in absorbance of each reaction mixture at 420 nm using a UV/Vis spectrophotometer (DU-800 Nucleic Acids/Protein Analyzer, Beckman Coulter, Brea, CA, USA). One unit of enzyme activity was defined as the amount of enzyme required to oxidize 1 μmol of ABTS per minute. Each laccase activity assay was performed at least in triplicate.

### 2.5. Dye Decolorization

Full wavelength (325 nm to 800 nm) scanning of five synthesized dyes was performed using a UV/Vis spectrophotometer to record their maximal adsorbent peaks (Figure S2), which were used as the wavelength values for dye absorbance measurement. Decolorization by bacCTS-MB1 was assessed using a previously described method with some modifications. First, 2 g of each bacCTS-MB1 complex was added to a 10-mL reaction system containing 8.5 mL of 0.1 mol $L^{-1}$ sodium acetate buffer (pH 2.5), 0.5 mL of 2 mmol $L^{-1}$ $CuCl_2$ and 1.0 mL of dye at the final concentration of 1.0 g $L^{-1}$. Second, the absorbance of each reaction mixture supernatant was spectrophotometrically measured at the maximal absorbance wavelength value of each dye ($\lambda_{max}$) (Table S1 and Figure S2). Activity was expressed as the relative decolorization value, which was calculated as follows:

$$\text{Relative decolorization value}(\%) = \frac{(A_0 - A_f)}{A_0} \times 100\% \quad (1)$$

where $A_0$ denotes the initial absorbance value and $A_f$ denotes the final absorbance value.

For the ten-round repeated decolorization experiments, 2 g of each prepared bacCTS-MB1 complex was tested for AG25 decolorizing activity (final concentration of 1 g $L^{-1}$ AG25) in shake-flask trials in 10 mL of reaction solution at pH 2.5 and 25 °C with 180 rpm shaking. After each decolorization reaction round, the complex was harvested by centrifugation, repeatedly washed with $ddH_2O$ and then directly subjected to the next round of decolorization under similar decolorization reaction condition.

To examine the decolorizing activity of bacCTS-MB1 after a round of decolorization in conjunction with culturing for a generation, the supernatant was removed via centrifugation after a decolorization reaction, repeatedly washed with dd$H_2O$ until the supernatant no longer discolored, then 100 mL of LB broth were added directly into the flask, following by incubation at 25 °C for 4 h with 200 rpm of shaking. This procedure was not conducted under strict aseptic conditions. A next-round decolorization reaction was then carried out under similar reaction conditions. A total of six rounds of decolorization with five rounds of culturing for a generation were conducted. The decolorization activity of the bacCTS-MB1 complex with or without culturing for a generation was measured according to the procedures described above and the relative decolorization value of each reaction was calculated according to Formula (1).

### 2.6. Characterization of the CTS-MBs, aCTS-MBs and bacCTS-MBs

The particle sizes of all prepared CTS-MB materials were measured using a Zetasizer Nano-ZS (Malvern Instruments, Malvern, UK) with 100 randomly selected CTS-MBs from each preparation. The CTS-MB1, aCTS-MB1, bacCTS-MB1 and *P. putida* cell samples were dried using vacuum freeze-drying procedures. These samples were mixed with KBr, pressed into tablets and subjected to FT-IR spectral analyses using an FT-IR spectrometer (Spectrum One; PerkinElmer, Waltham, MA, USA). All infrared spectra were recorded within the 480–4000 $cm^{-1}$ spectral range. For the SEM observations of aCTS-MB1, bacCTS-MB1 and *P. putida* cell morphology, a small amount of each prepared sample was dehydrated using a series of gradient ethanol solutions (40%, 70%, 90% and 100%); subsequently, the samples were vacuum dried, gold coated using a sputter coater and then observed under a JSM-6390/LV SEM (NTC, Tokyo, Japan) following the manufacturer's instructions.

### 2.7. Data Analysis

Data analysis was performed using SPSS (Statistical Package for the Social Sciences) software, version 17.0. All data presented are the averages of at least three assays. Statistical significance was defined as $P < 0.05$.

## 3. Results and Discussion

### 3.1. Preparation and Characterization of the IBCC-B Complexes

Five CTS-MB materials with different particle sizes were prepared from a pulverous CTS substrate using a self-assembled device (Figure S1). With decreasing HV-PS voltage intensity values, the particle size of the prepared CTS-MBs increased continuously. As shown in Figure S3, all prepared CTS-MBs were uniform microspherical beads that were water-insoluble but well-compatible and well-dispersive in water. Among these CTS-MBs, the CTS-MB1 sample, which was prepared at the maximum working voltage (5.3 kV), had the smallest average particle size and largest average specific area compared to those of the other as-prepared materials; conversely, the CTS-MB5 sample prepared at 0 kV had the largest particle size and smallest average specific area.

The engineered *P. putida* cells with surface-displayed laccases were immobilized onto the CTS-MBs through immobilization reactions to construct dual-function biosorbent/biodegrading materials. To increase the immobilization efficiency, the as-prepared CTS-MB materials were initially modified with surface-grafted aldehyde groups, which allow *P. putida* immobilization via covalent crosslinking to the CTS-MBs in addition to electrostatic and physical adsorption. An orthogonal test at four factors/five levels with regard to the effects of glutaraldehyde concentration (0.5%, 1.0%, 2.0%, 5.0% and 8.0%,), reaction time (2, 4, 6, 8 and 12 h), temperature (4, 12, 16, 28 and 36 °C) and CTS-MB preparation (CTS-MB5 to CTS-MB1) was performed to optimize the immobilization reaction conditions based on the whole-complex laccase activity of each bacCTS-MB preparation (Table S2). Table S3 shows that the four factors exhibited an optimized effect on the CTS-MB-initiated immobilization of *P. putida* MB285 in the following order: reaction time > temperature > glutaraldehyde concentration >

CTS-MB particle size. The optimized factors corresponded to the combination "$B_3C_3A_5D_5$" (Table S3), indicating that the optimized treatment conditions were as follows: an immobilization reaction time of 6 h, a temperature of 20 °C and a glutaraldehyde concentration of 8% with the smallest particle-sized CTS-MB1.

Under the above optimized immobilization conditions, complexes bacCTS-MB1s were prepared by immobilizing *P. putida* cells onto CTS-MB1s. For comparison, four other complexes (bacCTS-MB2s, -MB3s, -MB4s and -MB5s) were also prepared in parallel using the CTS-MB2, CTS-MB3, CTS-MB4 and CTS-MB5 matrices, respectively. Figure S4 shows that the bacCTS-MB1s exhibited the highest whole-complex laccase enzyme activity as well as the highest immobilized count of *P. putida* cells, —it is apparently attributable to the smallest specific surface area of CTS-MB1 by which more *P. putida* MB285 cells were bound. Therefore, the bacCTS-MB1 complex was selected as the decolorization material for subsequent experiments.

The immobilization profiles of the bacCTS-MB1 complex, aCTS-MB1s and free *P. putida* MB285 cells were morphologically examined using SEM. The rugged and porous structures of the aCTS-MB1s (Figure 2A) were clearly observed and MB285 cells appeared in a naturally dispersed state (Figure 2B). However, the surface of the bacCTS-MB1 complex was covered by a large number of cells that formed clusters of cell aggregates (Figure 2C). These results indicated that during the formation of "CTS-MB/*P. putida* cells" as an integral composite, the surface-grafted aldehyde groups and porous and ion-charged surfaces of CTS-MB1 caused the immobilization of *P. putida* cells, which constitute an associative biomass.

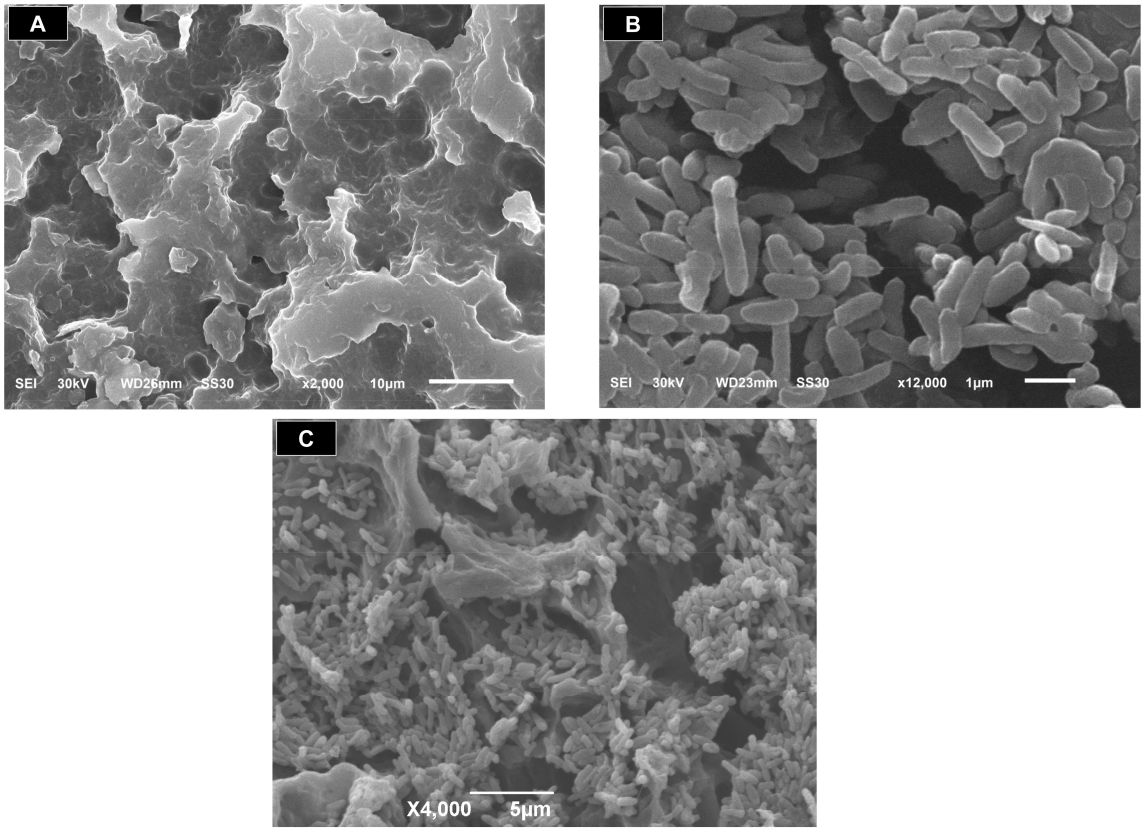


**Figure 2.** Representative SEM micrograph of the aCTS-MBs (**A**), *P. putida* MB285 cells (**B**) and the bacCTS-MB1 complex (**C**).

FT-IR spectroscopic analyses of free *P. putida* MB285 cells, CTS-MB1s, aCTS-MB1s and bacCTS-MB1s were performed to verify the chemical groups involved in the binding of the CTS-MBs and *P. putida* cells. Figure 3 shows the aCTS-MB1 spectrum in which the displayed peak at 1599 $cm^{-1}$ that represents the δ(N–H) bending vibration absorption peak of the aCTS-MB1s was

obviously weakened, whereas the $\nu$(C–N) stretching vibration absorption peak in the 1642–1658 $cm^{-1}$ region was increased significantly; no significant changes were found in the other absorption peaks, suggesting covalent binding between the aldehyde groups of glutaraldehyde and the amino groups. The bacCTS-MB1 spectrum displayed peaks at 1640, 1599 and 1310 $cm^{-1}$, which represent the $\nu$(C=O) stretching vibration absorption peak, the $\delta$(N–H) bending vibration absorption peak and the $\nu$(C–H) stretching vibration absorption peak, respectively; the latter two peaks were both somewhat weakened, indicating that the acylation in the bacCTS-MB1s was further weakened. Moreover, the ν(O-H) and $\nu$(N–H) stretching vibration absorption peak at 3430–3440 $cm^{-1}$ in the bacCTS-MB1 spectrum was also slightly weakened, which might be due to the binding of amino groups and aldehyde groups on the surface of the bacCTS-MB1s. These results indicated that the variance of surface groups on both the aCTS-MB1s and bacCTS-MB1s that result from surface-grafting modification and *P. putida* cell immobilization might be involved in the binding of cells to the surface of the CTS-MB1s.

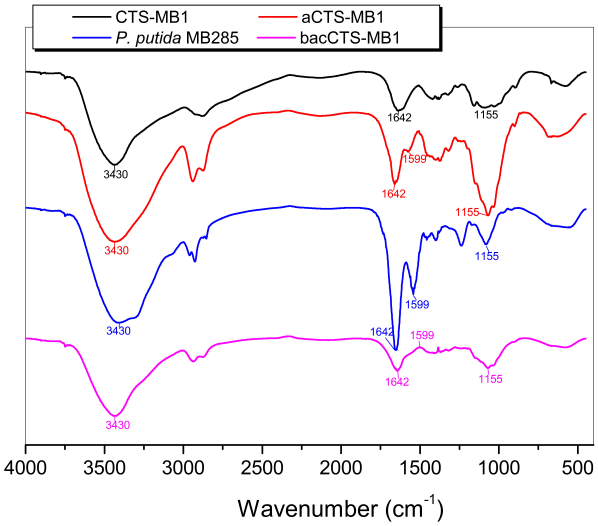


**Figure 3.** FT-IR spectra for *P. putida* MB285 cells and the as-prepared CTS-MB1s, aCTS-MB1s and bacCTS-MB1s.

### *3.2. Effects of Temperature, pH and Storage Time on the Laccase Activity of the bacCTS-MB1*

The effects of different temperatures on the whole-complex laccase activity of the bacCTS-MB1s and the whole-cell laccase activity of *P. putida* MB285 cells were comparatively examined at a range of 15 °C to 85 °C. As shown in Figure 4A, both the bacCTS-MB1s and MB285 cells exhibited parallel variation profiles along with increasing temperature. From 15 °C to 25 °C, the activity of the bacCTS-MB1s and MB285 cells increased rapidly, with maximum activity observed at 25 °C; however, their activity declined sharply at temperatures above 30 °C. Nevertheless, for the bacCTS-MB1 complex, a greater degree of thermostability was evident, as this enzyme lost only 46.4% of its activity at 55 °C, 52.3% at 65 °C and 83.2% at 75 °C, whereas the MB285 cells lost 57.8% of their enzyme activity at 55 °C, 72.6% at 65 °C and 94.8% at 75 °C. Therefore, the bacCTS-MB1 complex exhibited improved thermostability towards higher temperatures.

Figure 4B shows that although the pH range of the bacCTS-MB1 complex and *P. putida* cells extended from pH 1 to 7, the optimal pH value was 2.5, indicating that the cross-linking immobilization did not alter the optimal pH value of the *P. putida* MB285 laccase. Even at in a pH value range of 3 to 7, the bacCTS-MB1 complex retained more stable laccase activity compared to that of the free *P. putida* MB285 cells, suggesting a sheltering effect of the CTS-MB1 matrix on the immobilized cells, which led to the improved performance of the bacCTS-MB1s at higher pH values.

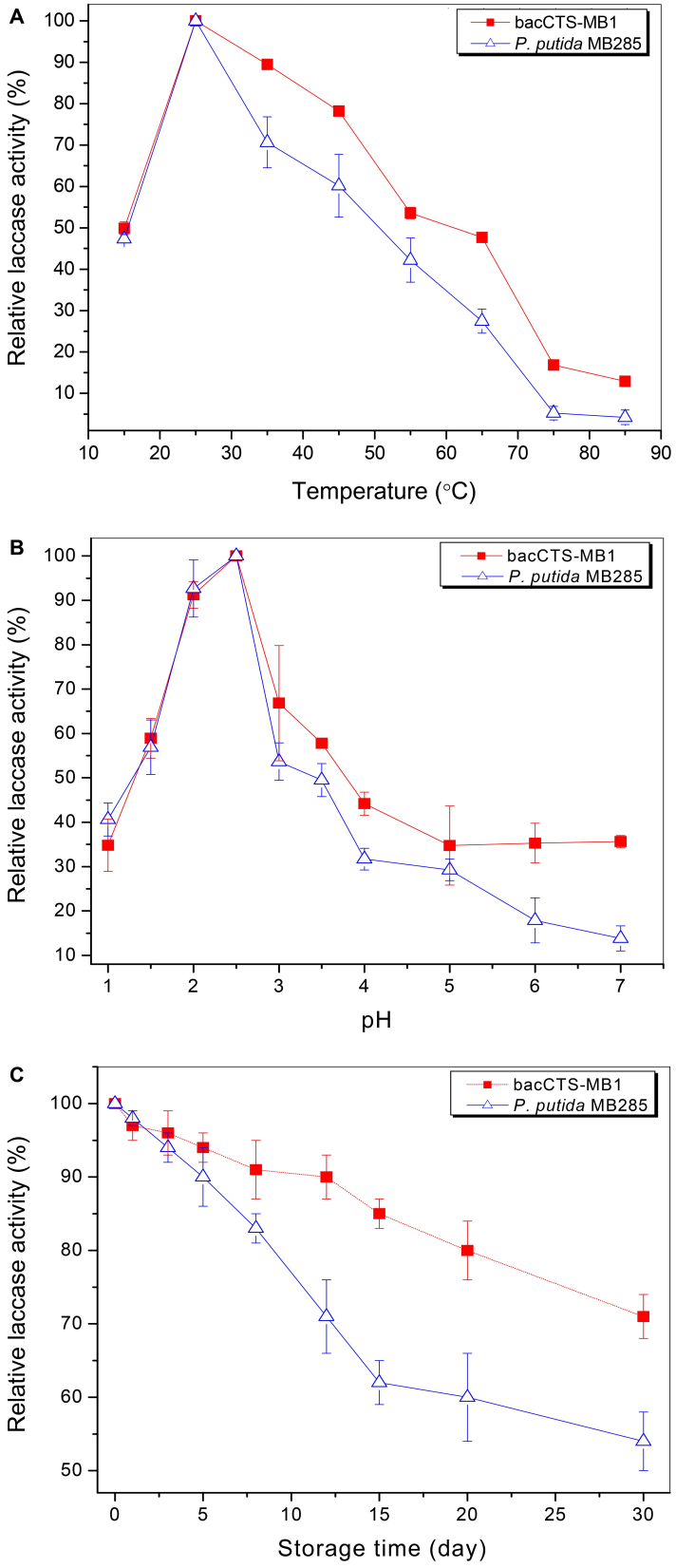


**Figure 4.** Effect of temperature (**A**), pH value (**B**) and storage time (**C**) on the whole-complex laccase enzyme activity of the bacCTS-MB1 complex. Whole-cell laccase enzyme activity of *P. putida* MB285 cells alone was assayed in parallel.

The bacCTS-MB1 complex and a *P. putida* MB285 cell suspension were stored at 4 °C for 30 days to monitor laccase activity attenuation. As shown in Figure 4C, the bacCTS-MB1 complex was more stable, retaining its enzyme activity over the 30 days of incubation, with the loss of only 15% of its activity at day 15, 20% at day 20 and 29% at day 30; conversely, the free *P. putida* MB285 cells lost 38% of their enzyme activity at day 15, 40% at day 20 and 46% at day 30. These results indicate that a CTS matrix platform is apparently conducive to retain the activity of *P. putida* MB285 cells with surface-displayed laccase enzymes.

### *3.3. Dye Decolorization by the bacCTS-MB1 Complex*

Prior to dye decolorization using the bacCTS-MB1 complex, single factor tests for reaction time, bacCTS-MB1 loading, pH, temperature and shaking speed with 1 g $L^{-1}$ of the representative anthraquinone dye AG25 and the azo dye AR18 were performed to optimize the degradation reaction conditions. The time-course patterns of AG25/AR18 decolorization were initially determined using 2 g of the bacCTS-MB1s under the following reaction conditions: pH 2.5, 25 °C and a shaking speed of 180 rpm (Figure 5A). The results showed that the decolorization of both AG25 and AR18 occurred rapidly, with approximately 90% of the reaction equilibrium value attained within the first 20 min and an increasing trend maintained until 30 min, at which time the final decolorization reaction equilibrium was reached. Therefore, 30 min set as the reaction time for the other factor experiments. Figure 5B shows that the decolorization of AG25 and AR18 using 2 g of the bacCTS-MB1s reached its maximal value in a 30-min reaction. Figure 5C,D show that the bacCTS-MB1s were capable of decolorizing AG25 and AR18 across a wide pH range of 2.5–8.5 and a relatively broad temperature range of 15–85 °C. At an optimal pH value of 2.5 and an optimal temperature of 25 °C, the decolorization reached its maximal value in 30 min. Figure 5E shows that shaking increased the decolorization reaction compared to static conditions, with every shaking speed increasing the relative decolorization rate. Although shaking at 240 rpm exhibited faster decolorization of AG25 compared with that of 180 rpm, both reached similar decolorization values of AG25 and AR18 in 30 min. Thus, the optimized decolorization reaction conditions were defined as follows: a reaction time of 30 min with a loading of 2 g of the bacCTS-MB1s at a pH of 2.5, a temperature of 25 °C and a shaking speed of 180 rpm.

The decolorization capacity of the bacCTS-MB1s on five industrial dyes was determined under optimized shake-flask incubation conditions. Figure 6 shows that the bacCTS-MB1 complex exhibited remarkable dye decolorization, with a maximum relative decolorization value of 96.2% for AG25, 95.6% for AR18, 96.3% for RB198, 95.7% for RB220 and 94.3% for DR243 in 30 min (Figure 6A); conversely, the cell-free CTS-MBs exhibited limited decolorization capacity with 29.0%, 28.7%, 16.2%, 36.0% and 21.9% decolorization values, respectively (Figure 6B). These results indicated that the immobilized *P. putida* MB285 cells contributed to the decolorization of dyes and the CTS-MB matrix subsidiarity increased the total decolorization capacity via its biosorption activity.

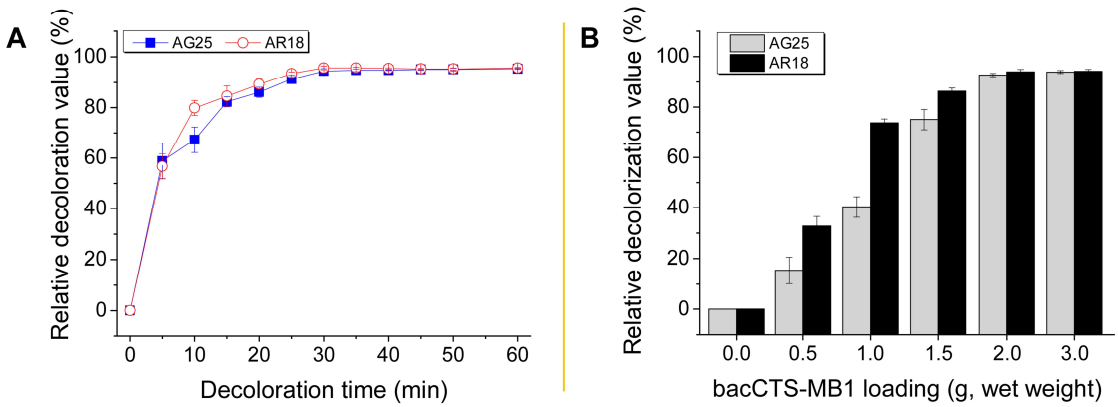


**Figure 5.** *Cont.*

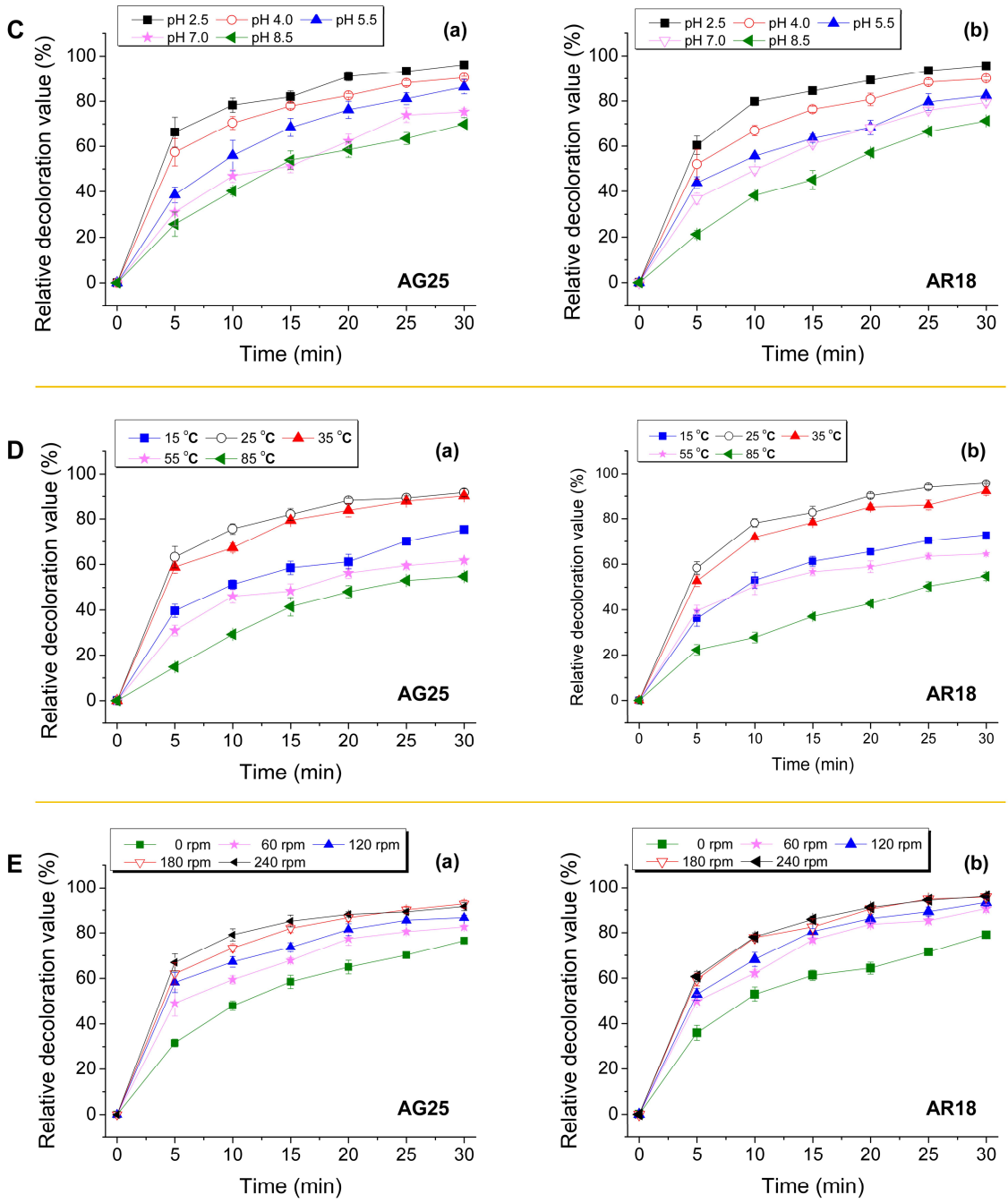


**Figure 5.** Effect of reaction time (**A**), bacCTS-MB1 loading (**B**), pH value (**C**), temperature (**D**) and shaking speed (**E**) on AG25 and AR18 decolorization by the IBCC-B1s. Each reaction included 2 g (unless otherwise specified) of the bacCTS-MB1s (wet weight) and a final concentration of 1 g $L^{-1}$ of the dye substrate.

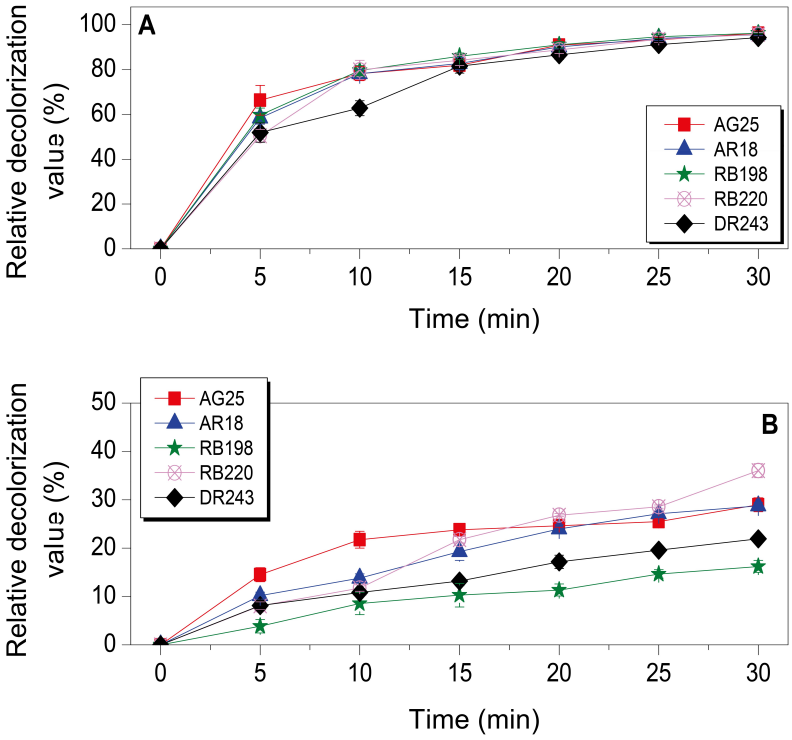


**Figure 6.** Dye decolorization of bacCTS-MB1s (**A**) and CTS-MB1s (**B**) towards AG25, AR18, RB198, RB220 and DR243. Decolorization was performed using 2 g of the bacCTS-MB1s or CTS-MB1s (wet weight) at 28 °C and pH 2.5 with shaking at 180 rpm for 30 min.

### *3.4. Effect of Repeated Use on AG25 Decolorization by the bacCTS-MB1s*

Figure 7 shows that the bacCTS-MB1 complex maintained substantial AG25 decolorization capacity with repeated use, retaining over 80% of its decolorization value after the first five rounds of repeated reactions, which represents a loss of only 13% in the 5th round compared to the first round. Although relatively rapid loss occurred from the 6th to the 10th round, the complex still retained a relative decolorization value of over 40%. These results reflected the strong viability of *P. putida* MB285 cells under such treatments, thereby suggesting that the bacCTS-MB1s have good persistent efficacy during decolorization of the AG25 dye.

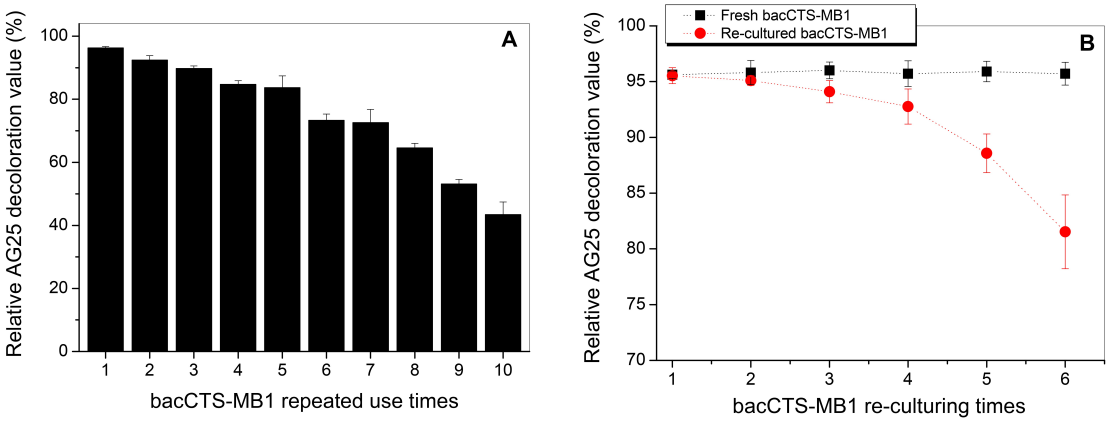


**Figure 7.** AG25 decolorization capacity of the bacCTS-MB1s during continuously repeated reactions (**A**) and during continuous decolorization and re-culturing cycles (**B**). In (**B**), equivalent freshly prepared bacCTS-MB1s were used as a control for each decolorization reaction cycle.

### *3.5. Effect of Re-Culturing Time on Decolorization by the bacCTS-MB1s*

The re-culture and reusability of a dye-decolorizing material affects its potential for continuous decolorization processes. Six continuous rounds of AG25 decolorization and with re-culture were performed via shake flask trials to examine the effect of re-culture on the decolorization capacity of the bacCTS-MB1s. Figure 7B shows that the first four rounds of re-cultured bacCTS-MB1s had a decolorization value approximately 8% greater than that of the directly used bacCTS-MB1 complex (Figure 7A), indicating that though effective, the re-culturing process was inappropriate during the first 3-4 rounds of use for the purpose of facile and fast material retrieval.

## 4. Conclusions

The present study reports a new decolorization material that is capable of decolorizing different kinds of dyes with high capacity and improved physical strength for potential applications in large-scale or continuous operations. Following the preparation of CTS-MBs using a self-configuring device, engineered *P. putida* MB285 cells with surface-displayed laccases were immobilized mainly through covalent cross-linkages, thus forming a degrading-biosorption bifunctional complex. SEM and infrared analysis confirmed the successful immobilization of the cells onto the CTS-MB matrix. The prepared complexes with maximum whole-complex enzyme activity, bacCTS-MB1, was used to decolorize five industrially used dyes in shake flask trials. The results showed that this complex exhibited high decolorization capacity under the optimized reaction conditions. Moreover, the bacCTS-MB1 complex showed favorable activity with repeated and regenerated use. Therefore, the bacCTS-MB1 complex efficiently immobilized *P. putida* cells and demonstrated enhanced decolorization activity and improved physical strength. This system could be potential for further applications in large-scale or continuous processes; however, the feasibility of this system must be validated in naturally occurring, polluted bodies of water where various dyes and other pollutants coexist and could cause interference. The development of an applicable system based on the bacCTS-MB1s to treat industrial dye-polluted waters will be our next primary research goal.

**Supplementary Materials:** The following are available online at http://www.mdpi.com/2076-3417/9/1/138/s1, Figure S1: Schematic illustration of the self-assembled facile device for the preparation of various CTS-MBs with different particle sizes; Figure S2: Morphological images of the five as-prepared CTS-MB materials and their average diameters and specific surface area values; Figure S3: Full wavelength (325 nm to 800 nm) scanning curves of five synthesized dyes indicating their maximal adsorbent peaks (arrows), which were used as the OD values for the dye absorbance measurements; Figure S4: Whole-composite laccase enzyme activity and immobilized *P. putida* cell counts of the five prepared bacCTS-MB materials; Table S1: Molecular formulas of five selected synthesized dyes; Table S2: $L_{25}$ ($4^5$)-orthogonal test of *P. putida* MB285 immobilization on the CTS-MBs; Table S3: Significance analysis of the factors in the $L_{25}$-orthogonal test of *P. putida* MB285-immobilization.

**Author Contributions:** Z.B., X.S. and X.Y. performed the experiments. Z.B. drafted the manuscript. L.L. conceived and directed the study and revised the manuscript.

**Funding:** This work was funded by the National Natural Science Foundation of China (Grant No. 31570123 and 31770108) and the Fundamental Research Funds for the Central Universities (Program No. 2662015PY189).

**Conflicts of Interest:** The authors declare no conflict of interest.

## References

1. Husain, Q. Potential applications of the oxidoreductive enzymes in the decolorization and detoxification of textile and other synthetic dyes from polluted water: A review. *Crit. Rev. Biotechnol.* **2006**, *26*, 201–221. [CrossRef] [PubMed]
2. Srinivasan, A.; Viraraghavan, T. Decolorization of dye wastewaters by biosorbents: A review. *J. Environ. Manag.* **2010**, *91*, 1915–1929. [CrossRef] [PubMed]
3. Cheng, S. Heavy metal pollution in China: Origin, pattern and control. *Environ. Sci. Pollut. Res. Int.* **2003**, *10*, 192–198. [CrossRef]

4. Dos Santos, A.B.; Cervantes, F.J.; van Lier, J.B. Review paper on current technologies for decolourisation of textile wastewaters: Perspectives for anaerobic biotechnology. *Bioresour. Technol.* **2007**, *98*, 2369–2385. [CrossRef] [PubMed]
5. Nidheesh, P.V.; Gandhimathi, R.; Ramesh, S.T. Degradation of dyes from aqueous solution by Fenton processes: A review. *Environ. Sci. Pollut. Res. Int.* **2013**, *20*, 2099–2132. [CrossRef] [PubMed]
6. Muxika, A.; Etxabide, A.; Uranga, J.; Guerrero, P.; de la Caba, K. Chitosan as a bioactive polymer: Processing, properties and applications. *Int. J. Biol. Macromol.* **2017**, *105*, 1358–1368. [CrossRef]
7. Farzana, M.H.; Meenakshi, S. Photo-decolorization and detoxification of toxic dyes using titanium dioxide impregnated chitosan beads. *Int. J. Biol. Macromol.* **2014**, *70*, 420–426. [CrossRef]
8. Bilal, M.; Asgher, M.; Iqbal, M.; Hu, H.; Zhang, X. Chitosan beads immobilized manganese peroxidase catalytic potential for detoxification and decolorization of textile effluent. *Int. J. Biol. Macromol.* **2016**, *89*, 181–189. [CrossRef]
9. Lin, Y.H.; Lin, W.F.; Jhang, K.N.; Lin, P.Y.; Lee, M.C. Adsorption with biodegradation for decolorization of reactive black 5 by Funalia trogii 200800 on a fly ash-chitosan medium in a fluidized bed bioreactor-kinetic model and reactor performance. *Biodegradation* **2013**, *24*, 137–152. [CrossRef]
10. Wang, J.; Chen, C. Chitosan-based biosorbents, modification and application for biosorption of heavy metals and radionuclides. *Bioresour. Technol.* **2014**, *160*, 129–141. [CrossRef]
11. Philibert, T.; Lee, B.H.; Fabien, N. Current status and new perspectives on chitin and chitosan as functional biopolymers. *Appl. Biochem. Biotechnol.* **2017**, *181*, 1314–1337. [CrossRef] [PubMed]
12. Thakur, V.K.; Voicu, S.I. Recent advances in cellulose and chitosan based membranes for water purification: A concise review. *Carbohydr. Polym.* **2016**, *146*, 148–165. [CrossRef]
13. Yang, R.; Li, H.; Huang, M.; Yang, H.; Li, A. A review on chitosan-based flocculants and their applications in water treatment. *Water Res.* **2016**, *95*, 59–89. [CrossRef]
14. LogithKumar, R.; KeshavNarayan, A.; Dhivya, S.; Chawla, A.; Saravanan, S.; Selvamurugan, N. A review of chitosan and its derivatives in bone tissue engineering. *Carbohydr. Polym.* **2016**, *151*, 172–188. [CrossRef] [PubMed]
15. Muanprasat, C.; Chatsudthipong, V. Chitosan oligosaccharide: Biological activities and potential therapeutic applications. *Pharmacol. Ther.* **2017**, *170*, 80–97. [CrossRef] [PubMed]
16. Canas, A.I.; Camarero, S. Laccases and their natural mediators: Biotechnological tools for sustainable eco-friendly processes. *Biotechnol. Adv.* **2010**, *28*, 694–705. [CrossRef] [PubMed]
17. Ba, S.; Vinoth Kumar, V. Recent developments in the use of tyrosinase and laccase in environmental applications. *Crit. Rev. Biotechnol.* **2017**, *37*, 819–832. [CrossRef] [PubMed]
18. Claus, H. Laccases and their occurrence in prokaryotes. *Arch. Microbiol.* **2003**, *179*, 145–150. [CrossRef]
19. Claus, H. Laccases: Structure, reactions, distribution. *Micron* **2004**, *35*, 93–96. [CrossRef]
20. Bertrand, B.; Martinez-Morales, F.; Trejo-Hernandez, M.R. Upgrading laccase production and biochemical properties: Strategies and challenges. *Biotechnol. Prog.* **2017**, *33*, 1015–1034. [CrossRef]
21. Chauhan, P.S.; Goradia, B.; Saxena, A. Bacterial laccase: Recent update on production, properties and industrial applications. *3 Biotech* **2017**, *7*, 323. [CrossRef] [PubMed]
22. Chen, Y.; Stemple, B.; Kumar, M.; Wei, N. Cell surface display fungal laccase as a renewable biocatalyst for degradation of persistent micropollutants bisphenol A and sulfamethoxazole. *Environ. Sci. Technol.* **2016**, *50*, 8799–8808. [CrossRef] [PubMed]
23. Couto, S.R.; Toca-Herrera, J.L. Industrial and biotechnological applications of laccass: A review. *Biotechnol. Adv.* **2006**, *24*, 500–513. [CrossRef] [PubMed]
24. Peralta-Zamora, P.; Pereira, C.M.; Tiburtius, E.R.L.; Moraes, S.G.; Rosa, M.A.; Minussi, R.C.; Durán, N. Decolorization of reactive dyes by immobilized laccase. *Appl. Catal. B Environ.* **2003**, *42*, 131–144. [CrossRef]
25. Wang, W.; Zhang, Z.; Ni, H.; Yang, X.; Li, Q.; Li, L. Decolorization of industrial synthetic dyes using engineered *Pseudomonas putida* cells with surface-immobilized bacterial laccase. *Microb. Cell Fact.* **2012**, *11*, 75. [CrossRef] [PubMed]
26. Shao, X.; Gao, Y.; Jiang, M.; Li, L. Deletion and site-directed mutagenesis of laccase from *Shigella dysenteriae* results in enhanced enzymatic activity and thermostability. *Enzyme Microb. Technol.* **2009**, *44*, 274–280. [CrossRef]

27. Ramos, J.L.; Sol Cuenca, M.; Molina-Santiago, C.; Segura, A.; Duque, E.; Gomez-Garcia, M.R.; Udaondo, Z.; Roca, A. Mechanisms of solvent resistance mediated by interplay of cellular factors in *Pseudomonas putida*. *FEMS Microbiol. Rev.* **2015**, *39*, 555–566. [CrossRef]
28. Kim, J.; Park, W. Oxidative stress response in *Pseudomonas putida*. *Appl. Microbiol. Biotechnol.* **2014**, *98*, 6933–6946. [CrossRef]
29. El Kadib, A. Chitosan as a sustainable organocatalyst: A concise overview. *ChemSusChem* **2015**, *8*, 217–244. [CrossRef]
30. Krajewska, B. Application of chitin- and chitosan-based materials for enzyme immobilizations: A review. *Enzyme Microb. Technol.* **2004**, *35*, 126–139. [CrossRef]
31. Chiou, M.S.; Chuang, G.S. Competitive adsorption of dye metanil yellow and RB15 in acid solutions on chemically cross-linked chitosan beads. *Chemosphere* **2006**, *62*, 731–740. [CrossRef] [PubMed]
32. Sambrook, J.; Russell, D.W. *Molecular Cloning: A Laboratory Manual*, 3rd ed.; Cold Spring Harbor Laboratory Press: Cold Spring Harbor, NY, USA, 2001.